Self-diffusion and collective diffusion in a model viscoelastic system

Eric Michel,[1] Luca Cipelletti,[1,*] Emmanuel d'Humieres,[2] Yann Gambin,[2] Wladimir Urbach,[2] Grégoire Porte,[1] and Jacqueline Appell[1]

[1]*Groupe de Dynamique des Phases Condensées (UMR 5581), Université Montpellier 2, 34095 Montpellier Cedex 5, France*

[2]*Laboratoire de Physique Statistique de l'Ecole Normale Supérieure, 24 rue Lhomond, F-75231 Paris Cedex 05, France*

(Received 7 April 2002; published 10 September 2002)

We use dynamic light scattering (DLS) and fluorescence recovery after pattern photobleaching (FRAPP) to investigate the dynamics of a model transient network made of an oil-in-water droplet microemulsion to which small amounts of a telechelic polymer are added. The DLS correlation functions exhibit three relaxation modes. The two first modes can be interpreted quantitatively in the frame of the classical De Gennes–Brochard theory of DLS in viscoelastic system. The third, slower mode is diffusive and arises from the ternary character (droplets, polymers, and water) of the system. By contrast, the pattern relaxation in FRAPP exhibits a single-, slow-exponential decay with a characteristic time proportional to the squared inverse scattering vector: the corresponding self-diffusion coefficient of the droplets is found to be close to the diffusion coefficient characterizing the third mode in DLS. We interpret these results in terms of the coupled relaxation of the concentration fluctuations of the polymers and the droplets.

DOI: 10.1103/PhysRevE.66.031402 PACS number(s): 82.70.−y, 83.80.Kn, 78.35.+c

I. INTRODUCTION

In the late seventies, Brochard and De Gennes initiated a theory of the dynamic light scattering (DLS) by semidilute solutions of polymers [1,2]. This theory has been generalized to all viscoelastic media characterized by an instantaneous elastic modulus G_0 and a terminal time τ_R [3–6]. It is presently often referred to as the two-fluids theory. Two relaxation processes are predicted for the autocorrelation functions, as well as the variations of their characteristic times and amplitudes with the scattering vector q. These two modes are due to the coupling of the concentration fluctuations to the viscoelasticity of the system. Careful experimental check was reported by Adam and Delsanti [6], and later on by Nicolai *et al.* [7] who worked on viscoelastic solutions of entangled polystyrene in cyclohexane at various concentrations. Viscoelastic solutions of telechelic ionomers in oil (Johannson *et al.* [8]) were also investigated recently. In these works, reasonably good quantitative agreement between the experiments and the predictions of the two-fluids theory was generally found.

Among other viscoelastic systems, the ternary systems forming transient networks first studied by Gradzielsky [9] are specially interesting: unlike the binary system of Johansson *et al.* [8], it is possible to control separately the number density of the vertices of the network and their average connectivity. These systems consist of telechelic polymers with hydrophobic stickers grafted at the two ends, incorporated in an oil-in-water droplet microemulsion (see Fig. 1 for a schematic illustration). The hydrophobic stickers adsorb reversibly onto the oil droplets, and the polymers bridge or decorate the droplets, depending on whether the two stickers of a given polymer adsorb onto separate droplets or onto the same droplet. The viscoelasticity of the system depends on the number of bridging polymers (inverse systems consisting of a water-in-oil microemulsion and hydrophobic polymers with hydrophilic stickers have also been used). Several dynamic light scattering studies have been reported dealing with such ternary systems [10–13].

As discussed in Ref. [11], three dynamic relaxation modes (rather than two) are to be expected for such ternary systems, due to the presence of two distinct solute species (the polymers and the droplets). Indeed, three internal variables are needed to describe completely any given microstate of the system: the droplet concentration, the telechelic polymer concentration, and the links-to-loops ratio, i.e., the fraction of polymers that link distinct droplets rather than forming a loop around the same droplet. The link-to-loop ratio is an important quantity for determining the transient elastic properties of the system, since only polymers linking distinct droplets do contribute to the elasticity of the network. Both the droplet and the polymer concentrations are conserved variables: local changes in polymer or droplet concentrations are possible only through transport of matter. The corresponding "pure" modes (at fixed values of the two other internal variables) are expected to be diffusive. On the other hand, the links-to-loops ratio is a nonconserved variable, since local changes of this quantity do not involve transport of matter. The characteristic time of the mode associated to it

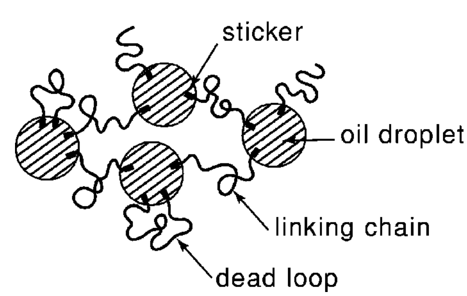

FIG. 1. Schematic representation of microemulsion droplets linked or decorated by telechelic chains. Only the bridging polymers contribute to the elasticity of the system.

*Electronic address: lucacip@gdpc.univ-montp2.fr

(at fixed values of the two other internal variables) is controlled by the residence time of the stickers and thus is expected to be q independent. We point out that the scattering from the polymers is negligible compared to that from the droplets: DLS only probes the fluctuations of the droplet concentration. However, these fluctuations are coupled to both the fluctuations of the polymer concentration and those of the links-to-loops ratio. Therefore, we indeed expect at least three relaxation modes in the correlation functions, these modes being linear combinations of the three pure modes described above.

In this respect, the results reported by Schwab and Stühn in Ref. [10] are particularly significant since they clearly show the existence of three distinct relaxation modes in such ternary mixtures: only the faster and the slower ones are diffusive, the intermediate having a characteristic time essentially independent of the scattering vector. The analogies in the polymer concentration dependence of this intermediate mode and that of the terminal stress relaxation time led the authors to identify it as the characteristic lifetime of a droplet as a junction. This intermediate mode is indeed to be identified with the viscoelastic mode of the De Gennes–Brochard theory. The fast mode is interpreted as the overdamped gel mode of the transient network. Finally, pulsed field gradient and nuclear magnetic resonance measurements revealed the existence of a slow self-diffusion of the telechelic polymer, whose diffusion coefficient is very close to that associated to the third, slow relaxation observed for DLS.

In a previous paper [11], we reported on rheology and DLS experiments in a ternary system very similar to that studied by Schwab and Stühn. However, we could find only two relaxation modes in the DLS correlation functions at all considered scattering vectors. The faster mode is clearly diffusive, while the slower mode is almost q independent. Moreover, the relative amplitudes of the two modes are found to be independent of q. These results are in good quantitative agreement with the De Gennes–Brochard theory [1,2] in the limit of a viscoelastic time very long compared to the diffusion time. On the other hand, the absence of a third relaxation time is intriguing when compared to the results of Schwab and Stühn and when considering the elementary analysis recalled above. Two hypothesis can be considered to explain the absence of the third mode: either the relative intensity of the third relaxation process is too small (very weak coupling between the polymer and droplet concentrations), or its characteristic time may be too long to be accessible to conventional dynamic light scattering experiments.

In order to clarify this point, we compare the behavior of the system studied in Ref. [11] to that of a similar system, for which the residence time of the hydrophobic stickers is reduced by a factor of order 10^3, all others parameters remaining unchanged. The characteristic time of the second relaxation mode, which is strongly related to the residence time of the stickers in the droplets, and that of the third relaxation mode—if it exists—are expected to be reduced accordingly by about three orders of magnitude. Indeed, for this system we observe a third, slow mode in the correlation function for all the concentrations of polymer. Its inverse characteristic times varies linearly with the squared scattering vector and an effective diffusion coefficient D_p can therefore be calculated, which we compare to the self-diffusion coefficient D_s of the droplets as measured by fluorescence recovery after pattern photobleaching (FRAPP). Both diffusion coefficients are very similar suggesting that the third mode in DLS be indeed controlled by the self-diffusion of the droplets. We argue, according to the general analysis above, that this signature of self-diffusion in DLS arises from the ternary character of the system where the interdiffusion of droplets and polymer are coupled to one another.

II. EXPERIMENTAL SYSTEM

The system is very similar to that described in Ref. [11]. It is composed of an oil-in-water droplet microemulsion, to which telechelic polymers are added. The microemulsion consists of decane droplets stabilized by a surfactant/cosurfactant monolayer (Triton X35 and Triton X100, in a weight ratio TX35/TX100 $=0.5$ w/w; the amount of decane is fixed so that decane/TX $=0.7$ w/w). The radius (82 Å) of the microspheres remains unchanged in a large range of droplet and polymer concentrations, as it has been shown by neutron scattering [14,15]. The polymers are polyethyleneoxide (PEO, molecular weight 10 k Dalton, polidispersity from 1.1 to 1.3, depending on the batch), grafted at the two ends with aliphatic chains of twelve (C12 samples, this work) or eighteen (C18 samples, Ref. [11]) carbon atoms, respectively; the end groups (stickers) adsorb reversibly onto the microemulsion droplets. The fluorescent dye utilized for the FRAPP experiments, five-octadecanoylaminofluorescein, has the same structure as a surfactant molecules: an aliphatic tail and a polar head. Its hydrophobic part, composed of 17 carbon atoms, adsorbs onto the droplets. The amount of dye dissolved in the microemulsion is small enough to have less than one dye molecule per droplet. We have checked by DLS on the bare microemulsion that the addition of the fluorescent dyes does not modify the hydrodynamic radius of the droplets.

Three parameters of the system can be controlled separately: the droplet concentration (volume fraction ϕ), the polymer concentration (we denote r the average number of stickers per droplet), and the residence time of the stickers in the droplets, which is determined by the chain length of the aliphatic end group. The residence time t_0 is related to the adhesion energy W of the stickers by the usual Arrhenius law: $t_0 = w_0^{-1}\exp(W/k_BT)$, where w_0 is an attempt frequency of the order of the inverse self-diffusion time of the sticker. For an aliphatic group in alcane, we expect W to be of the order of 1.2 to 1.5 k_BT per CH_2, based on the comparison of the critical micellar concentration (CMC) of omologous series of surfactants with various chain lengths [16]. Thus, the residence time of a 12-carbon sticker inside a droplet is expected to be about 10^3 to 10^4 times shorter than that of an 18-carbon sticker. To obtain an independent value of the ratio of the residence times for C18 and C12 samples, we have measured their low-shear viscosity η. For $\phi = 17.1\%$ and $r = 7$, we find $\eta = 38$ Pa s (C18) and $\eta = 0.028$ Pa s (C12). Since the connectivity of the two samples, and hence their instantaneous elastic modulus, does not depend on the sticker chain length, the ratio of their viscosities directly yields the ratio of the residence times. We find $t_0(\mathrm{C18})/t_0(\mathrm{C12}) = 1360$, in good agreement with the value estimated from the CMC data.

For all data presented in this work, the droplet volume fraction is $\phi = 17.1\%$. At this concentration, the mean inter-droplet separation is very close to the mean end-to-end distance of a free PEO chain in water (80 Å). Therefore, we expect the system to undergo a percolation transition as the polymer concentration is increased, without any significant changes in its structure. Indeed, above $r = 3.1$ (the percolation threshold), the C18 samples exhibit a power-law increase of their viscoelastic response [11,15]. Step strain relaxation experiments reveal a Maxwellien behavior, the elastic modulus $G(t)$ decaying nearly exponentially: $G(t) = G_0 \exp[-(t/\tau_R)^p]$, where G_0 is the instantaneous elastic modulus, and t_R the stress relaxation time. The exponent p is very close to one for all samples far above the percolation threshold. The stress relaxation time τ_R is related to the residence time of a sticker in a droplet, and is of the order of a few 10^{-1} s for the C18 samples (0.125 s for the sample with $r = 12.5$). For the C12 samples, on the contrary, τ_R is expected to be more than three orders of magnitude smaller, far below the time resolution of the rheometer (20 ms). Therefore, only the low-rate viscosity can be measured and the percolation threshold cannot be readily determined. In fact, even above the percolation threshold, the renewal time of the infinite size cluster of linked droplets is faster than the time resolution of the rheometer: therefore, the sharp onset of the viscoelasticity at the percolation threshold observed for the C18 samples is not seen with the C12 samples. A percolation threshold, however, must exist also for the latter samples, roughly at the same position in the ϕ vs r phase diagram as for the C18 samples [11]: percolation is a geometrical property of the network, and changes in the dynamic properties of the sample do not affect the geometry. Furthermore, the curves showing the macroscopic viscosity as a function of r (see Fig. 6 below) are not incompatible with the presence of a percolation threshold close to that measured in the C18 samples [11].

III. RESULTS AND DISCUSSION

A. Dynamic light scattering

Light scattering measurements were performed on a standard setup. The sample is placed at the center of a thermostated AMTEC goniometer, and is illuminated by an argon ion laser ($\lambda = 514.5$ nm). A Brookhaven BI9400 correlator is used to calculate the normalized time autocorrelation function of the scattered intensity, $g_2(t)$, which is related to the normalized autocorrelation function $g_1(t)$ of the scattered electric field by means of the Siegert relation $g_2(t) - 1 = \beta |g_1(t)|^2$, where β $(0 < \beta < 1)$ depends on the geometry of the setup. As recalled above, in our samples the scattering is dominated by the contribution of the droplets, and $g_1(t)$ is related to the autocorrelation function of the droplet concentration. Light scattering measurements thus probe the time fluctuations of the droplet concentration.

Figure 2(a) shows on a double logarithmic scale a typical

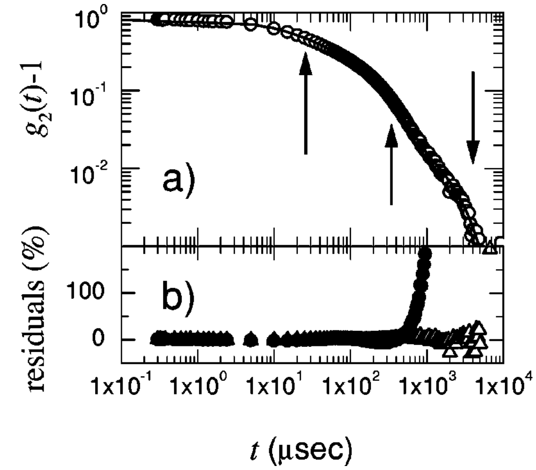

FIG. 2. (a) Autocorrelation function measured at $q = 3.14 \times 10^7$ m^{-1} for a sample with $r = 13.2$ and $\phi = 17.1\%$. The line is the fit by a sum of three-exponential decays; the arrows indicate the three relaxation times, $\tau_f = 23$ ms, $\tau_s = 264.1$ ms, and $\tau_p = 2974.3$. (b) Fit residuals for the sum of three- (open triangles) and two- (full circles) exponential decays, respectively.

autocorrelation function for a sample with $\phi = 17.1\%$ and $r = 13.2$ (open circles). The data can be very well fitted by the sum of three-exponential decays (solid line), whose characteristic times τ_f, τ_s, and τ_p are indicated by the arrows: $g_2(t) - 1 = [\alpha_f \exp(-t/\tau_f) + \alpha_s \exp(-t/\tau_s) + \alpha_p \exp(-t/\tau_p)]^2$. In order to demonstrate unambiguously the existence of three distinct relaxation processes, we show in Fig. 2(b) the fit residuals (percentage difference between the experimental data and the fit) when fitting to the data a two-exponential decay (solid circles) or a three-exponential decay (open triangles). While both fitting functions model equally well the data at short times, it is clear that for $t > 100$ ms a three-exponential decay is needed to capture correctly the full relaxation of $g_2(t) - 1$. We point out that for all the investigated samples ($\phi = 17.1\%$ and $4.4 \leqslant r \leqslant 17.6$) three relaxation modes are observed in the correlation functions, the contribution of the slowest mode increasing with r.

Remarkably, the two fastest modes are well described by the Brochard–de Gennes two-fluids theory. Figure 3 shows, for the same sample as in Fig. 2, the inverse relaxation times of the two modes as a function of the squared scattering vector (open symbols), while the solid lines are the simultaneous fits to the two set of data of the following expression, issued from the Brochard–De Gennes theory:

$$\tau_{f(s)}^{-1} = \frac{\tau_R^{-1} + D_{eff} q^2}{2} \times \left(1 \pm \sqrt{1 - \frac{4 D_{coll} q^2 \tau_R^{-1}}{(\tau_R^{-1} + D_{eff} q^2)^2}} \right), \tag{1}$$

where the sign plus (minus) in front of the square root refers to τ_f^{-1} (τ_s^{-1}). Here, D_{col} is the ϕ-dependent diffusion coefficient of the droplets in the absence of viscoelasticity, $D_{eff} = D_{col} + D_{el}$, where D_{el} is an effective "elastic" diffusion coefficient and τ_R is the terminal stress relaxation time as measured by rheometry. The elastic diffusion coefficient depends on the instantaneous elastic modulus of the sample

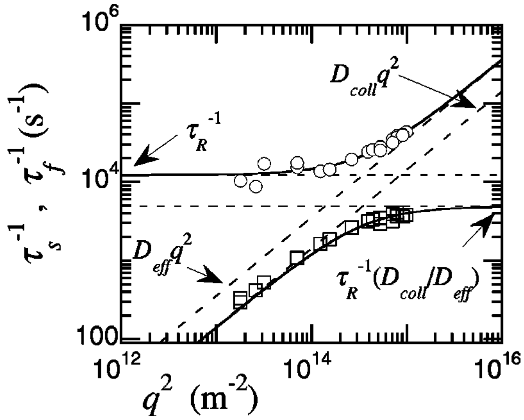

FIG. 3. Inverse faster, τ_f, and intermediate, τ_s, relaxation time vs squared scattering vector. The solid lines are the fit of the two-fluids theory Eq. (1) to the data. The dotted lines represent the asymptotic behavior at small and large q (hydrodynamic and gel regime, respectively).

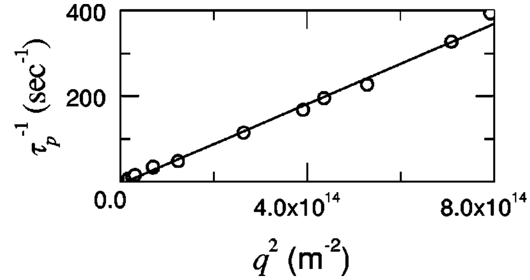

FIG. 4. Squared-q dependence of the inverse relaxation time of the slowest DLS mode. The line is a linear fit to the data yielding $D_p = 4.57\times10^{-13}$ m^2 s^{-1}.

G_0: $D_{el} = 4G_0\nu/n_0$, where $n_0 = \phi/(\frac{4}{3}\pi R^3)$ is the droplet number concentration and $\nu = (6\pi\eta_s R)^{-1}$ is the droplet mobility, with η_s the solvent viscosity and R the droplet radius.

As can be seen in Fig. 3, the quality of the fit is very good: the model describes well the experimental data. Note that for this system the range of q investigated falls at the crossover between the regime dominated by diffusion ($q^2 > \tau_R/D_{eff}, \tau_f^{-1} \approx D_{eff}q^2$) and that dominated by the viscoelasticity ($q^2 < \tau_R/D_{eff}, \tau_f^{-1} \approx \tau_R^{-1}$). We compare in Table I the values of D_{eff}, D_{col}, and τ_R obtained for the C12 sample from the fit shown in Fig. 3 to the values measured for a C18 sample at the same ϕ and r. As recalled above, the residence time of a C18 sticker inside a droplet is expected to be more than three orders of magnitude longer than that of a C12 sticker. As the residence time increases, D_{col} and D_{eff} in Eq. (1) are not expected to change (because D_{el} depends on the instantaneous elastic response of the network), while τ_R increases proportionally to the residence time. Indeed, we find that the values of D_{col} and D_{eff} compare well for the two samples, while τ_R obtained from DLS for the C12 sample is found to be 1400 time shorter than the stress relaxation time measured by rheology for the C18 sample. This ratio between the residence times is in excellent agreement with the value 1360 obtained from rheology data and corresponds to a difference of $1.2k_BT$ per methyl group for the energy of adhesion of the stickers, in good agreement with the value reported in Ref. [16]. The data shown in Table I prove that the Brochard–de Gennes model describes remarkably well the first two modes of relaxation of this ternary system. On the other hand, the third mode that appears in Fig. 2(a) is not predicted by the two-fluids theory (which implicitly assumes a binary system). Moreover, this slow mode is diffusive, as shown by the linear dependence of τ_p^{-1} on q^2, Fig. 4. The diffusion coefficient associated to it, $D_p = (\tau_p q^2)^{-1}$, is smaller than D_{eff} and D_{col} calculated from the two first modes: it is related to the slowest relaxation process that occurs on large time and length scales. The question naturally arises of the physical origin of this third relaxation mode; its diffusive nature suggests that it be due to the self-diffusion of the droplets, whose Brownian motion is slowed down by the high effective viscosity of the network.

TABLE I. Comparison of the diffusion coefficients D_{eff} and D_{coll} issued from the fits of the de Gennes–Brochard model Eq. (1), for samples prepared with 12 carbon atoms stickers (C12) and 18 carbon atom stickers (C18). Last column: comparison of the value of τ_R measured by rheology for the C18 sample, and that calculated from dynamic light scattering experiments for the C12 sample.

Sample	D_{eff} (m^2 s^{-1})	D_{coll} (m^2 s^{-1})	τ_R(s)
C12	3.55×10^{-11}	1.43×10^{-11}	8.1×10^{-5} (DLS)
C18	3.30×10^{-11}	1.02×10^{-11}	0.12 (rheology)

To test this hypothesis, we calculate the apparent viscosity η_{DLS} of the effective medium in which the droplets are diffusing. From the Stokes-Einstein relation, one obtains $\eta_{DLS} = k_BT/6\pi D_p R$, where we take $R = 102$ Å, the hydrodynamic radius of the droplets as determined by DLS on a bare microemulsion ($r=0$) by extrapolating to $\phi = 0$. The values of η_{DLS} thus obtained are then compared to the macroscopic viscosity η of the sample as measured by standard rheometry. For $r = 4.4$, $\eta_{DLS} = 15$ mPa s and $\eta = 11.6$ mPa s, while for $r = 6.6$, $\eta_{DLS} = 21.4$ mPa s, to be compared to $\eta = 25.4$ mPa s. The agreement is quite good and suggests that, on long time scales, the system behaves as if the droplets were simply diffusing in a medium whose effective viscosity is comparable to the macroscopic viscosity (a more detailed comparison of η_{DLS} and η is shown in Fig. 6, which we discuss below).

B. FRAPP

For the sample investigated, DLS experiments probe the collective motion of the droplets. In order to better understand the dynamics of the sample, and, namely, the diffusive process associated to the slowest relaxation mode, we performed FRAPP experiments. This technique allows one to measure the self-diffusion coefficient of a fluorescent dye [17–19]; since in our experiments the dye molecules are adsorbed onto the droplets, FRAPP measurements directly yield the self-diffusion coefficient of the droplets. The sample is first illuminated by a high intensity fringe pattern

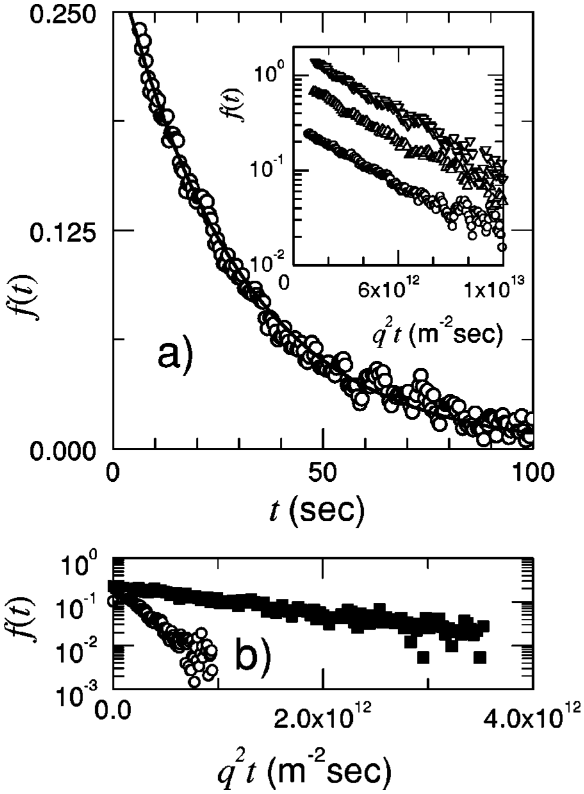

FIG. 5. (a) Main figure: typical FRAPP curve (fringe spacing $i=16$ μm). The line is a single-exponential fit to the data. Inset: semilogarithmic plot of the FRAPP signal vs tq^2 for various fringe spacings (from top to bottom, $i=11.43$, 6.25, and 16 μm). The data are parallel straight lines, indicating a diffusive behavior with $D_s=2.53\times10^{-13}$ m^{2}s^{-1}. (b) FRAPP signal vs tq^2 below ($r=1.1$, open circles) and above ($r=6.6$, solid squares) the percolation threshold: in both cases, the relaxation is a single exponential.

of spacing i. The droplets located in the dark fringes keep their fluorescence properties, whereas the dye molecules on the strongly illuminated droplets are bleached. The fluorescence recovery (i.e., the relaxation of the spatially periodic concentration profile of fluorescent dyes) is monitored by a low power laser beam, thereby probing the dynamics on a length scale i, corresponding to a scattering vector $q=2\pi/i$. The range of q accessible varies between 3.9×10^5 and 1×10^6 m^{-1} (fringe spacing ranging from 65 to 6.25 μm).

A typical FRAPP curve $f(t)$ for a connected microemulsion is shown in Fig. 5(a). The FRAPP signal (i.e., the normalized contrast of the fringe pattern after photobleaching) exhibits a single exponential decay with a characteristic time τ: $f(t)=A\exp(-t/\tau)$. In the inset, the FRAPP functions for various q are plotted vs tq^2 on a semilogarithmic scale. All the experimental data lie on parallel straight lines, showing that the single-exponential decay behavior holds for all fringe spacing (i.e., for all q), and that the inverse relaxation time varies proportionally to q^2. This behavior indicates that, on the large length scales probed by FRAPP, the motion of the droplets is diffusive, characterized by a q-independent self-diffusive coefficient $D_s=(\tau q^2)^{-1}$. The FRAPP data are thus in sharp contrast with the light scattering measurements, where three distinct relaxation processes are observed. A possible explanation for this difference could be that the relaxation of $f(t)$ arises from the diffusion of the dye jumping from one droplet to the next one, rather than from the diffusion of the droplets themselves. However, we point out that in order to prevent this eventuality a dye with a hydrophobic tail longer than that of the polymer stickers was chosen (17 carbon atoms instead of 12). Therefore, we expect the residence time of the dye to be roughly 400 times longer than that of the sticker and the FRAPP signal decay to be indeed determined by the motion of the droplets. Furthermore, we find that τ strongly depends on the connectivity r of the droplets, contrary to what would be expected if the relaxation of $f(t)$ was due to the hopping motion of the dyes from droplet to droplet.

In order to explain the single-exponential decay of $f(t)$, we note that the length scales probed by FRAPP are of the order of tens of micrometers, much larger than those probed by DLS. On such large length scales, the motion of the droplet over distances comparable to the size of the cage formed by its neighbors does not lead to an appreciable loss of contrast in the fringe pattern. Therefore, this motion, which is responsible for the two faster DLS modes, is not detected by FRAPP. By contrast, the long range motion resulting from the repeated escapes from a cage does eventually lead to the full mixing of the bleached and unbleached droplets, thus yielding the complete relaxation of the FRAPP signal. Therefore, the diffusive motion measured by FRAPP can be modeled by a random walk, whose elementary step is the process of escaping from one cage before being trapped in the next one.

Interestingly, FRAPP functions exhibit a single-exponential decay both below and above the percolation threshold, as shown in Fig. 5(b) (by comparison to the C18 samples, we estimate the percolation threshold to be at $r=3.1$ for the $\phi=17.1\%$ sample). The single-exponential behavior is indeed expected for a sample well above the percolation threshold, where the connectivity of the network is uniform: during equal time intervals, all droplets will cover on average equal distances, thus leading to a single-exponential relaxation of the FRAPP signal. On the contrary, such behavior is quite surprising below the percolation threshold, since the system is composed of separate clusters of connected droplets, whose size is widely distributed [20]. One could then argue that $f(t)$ be a stretched exponential, because each cluster would diffuse with a size-dependent diffusion coefficient and the FRAPP signal would reflect all these modes. However, we recall that the marked droplets are not permanently stuck to any given clusters, but rather they hop randomly from cluster to cluster many times during the fluorescence recovery. This movement of the droplets is superimposed to the diffusion of the aggregates. The single-exponential decay below the percolation threshold can then be understood in the following way: the shortest length scale probed by the FRAPP experiment is about 6 μm, more than 700 times the radius of a droplet. Therefore, any given droplet marked with a fluorescent dye explores several aggregates of different sizes during the fluorescence decay. Its dynamics is characterized by an effective diffusion coefficient which is, on average, the same for all dyes, thus leading to the single-

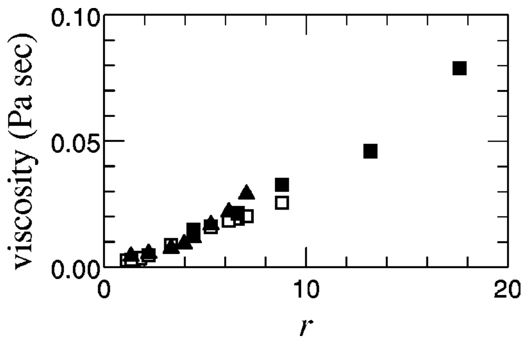

FIG. 6. r dependence of the viscosity measured by a Poiseuille viscometer (black triangles), and calculated from the diffusion coefficients D_p and D_s determined by DLS (full squares) and FRAPP (open squares), respectively.

exponential relaxation of $f(t)$.

The FRAPP data show that on length scales of tens of micrometers—much larger than the mean interdroplet distance—the motion of the microemulsion is diffusive. Since the system is homogeneous on such large length scales, we expect that, similarly to the case of the third relaxation mode observed by DLS, the effective viscosity associated to the diffusive motion of the droplets measured by FRAPP, η_{FRAPP}, be close to the macroscopic viscosity. In order to test this hypothesis, we show in Fig. 6 the r dependence of the macroscopic viscosity η (measured in a Poiseuille viscometer), together with η_{DLS} and η_{FRAPP}, obtained form D_p and D_s, respectively, via the Stokes-Einstein relation. As it can be seen, there is a good agreement between the three sets of data, thus indicating that the slowest relaxation mode in DLS, as well as the decay of the FRAPP signal, reflects the large length scale diffusionlike motion of the droplets. The microscopic origin of this motion is the cage-escaping process that continuously occurs as the stickers detach from one droplet and stick onto the next one. This very same process controls the flow properties of the system, thus leading to the good agreement between effective viscosity measured by DLS and FRAPP and the macroscopic viscosity.

In conclusion, the dynamics of ternary transient networks appear quite complex. In DLS, three modes are observed. The two fastest modes are very well described by the so called two-fluids model of viscoelastic media. The third, slow mode is diffusive; its characteristic time is quantitatively comparable to that of the self-diffusion of the droplets as measured by FRAPP. Following our analysis of the number of internal variables defining a given microstate of the system, we believe the existence of the third mode to arise from the ternary character of the network: the droplet concentration and the polymer concentration are thermodynamically coupled internal variables. In this framework, all three modes correspond to a separate step for the complete relaxation of the droplet concentration fluctuations. At short time (shorter than the residence time of the stickers), both the local connectivity and the local polymer-to-droplet ratio are transiently frozen: the first mode therefore corresponds to a partial relaxation at quenched connectivity and quenched polymer-to-droplet ratio (overdamped phonons of the elastic network). At intermediate time (longer than the sticker residence time but still shorter than the interdiffusion time of droplets and polymers), the local connectivity is relaxed (the transient elasticity is forgotten), but the local polymer-to-droplet ratio is still frozen. The second mode thus corresponds to further relaxation at annealed connectivity but quenched local polymer-to-droplet ratio. Finally, at times longer than the interdiffusion time of droplets and polymers, the local polymer-to-droplet ratio is also released by interdiffusion. The third mode then corresponds to the final step of the relaxation at annealed connectivity and local polymer-to-droplet ratio. The two first modes are related to droplets and polymers moving together. The third mode is determined by the relative motions of polymers and droplets, which we intuitively expect to have a kinetic of the order of the self-diffusion of the droplets in the viscoelastic background, as observed in the FRAPP experiments.

ACKNOWLEDGMENTS

We thank N. Tsapis for help in the FRAPP measurements, R. Aznar for synthesizing excellent quality C12 and C18 telechelic polymers, and T. Canzoneri for technical assistance in optimizing the detection of the DLS apparatus.

[1] F. Brochard and P.G. De Gennes, Macromolecules **10**, 1157 (1977).
[2] F. Brochard, J. Phys. Colloq. **44**, 39 (1983).
[3] U. Genz, Macromolecules **27**, 3501 (1994).
[4] C.H. Wang, J. Chem. Phys. **95**, 3788 (1991).
[5] C.H. Wang, Macromolecules **25**, 1524 (1992).
[6] M. Adam and M. Delsanti, Macromolecules **49**, 1261 (1985).
[7] T. Nicolai, W. Brown, R.M. Johnsen, Macromolecules **23**, 1165 (1990).
[8] R. Johannson, C. Chassenieux, D. Durand, and T. Nicolai, Macromolecules **28**, 8504 (1995).
[9] M. Gradzielsky, A.H. Rauscher, and J. Hoffmann, J. Phys. IV Colloq. **65**, C1 (1993).
[10] M. Schwab and B. Stühn, J. Chem. Phys. **112**, 6461 (2000).
[11] E. Michel, M. Filali, R. Aznar, G. Porte, and J. Appell, Langmuir **16**, 8702 (2000).
[12] H.-F. Eicke, U. Hofmeier, C. Quellet, and U. Zölzer, Prog. Colloid Polym. Sci. **90**, 165 (1992).
[13] G. Fleischer, F. Stieber, U. Hofmeier, and H.-F. Eicke, Langmuir **10**, 1780 (1994).
[14] M. Filali, R. Aznar, M. Svenson, G. Porte, and J. Appell, J. Phys. Chem. B **103**, 7293 (1999).
[15] M. Filali, M.J. Ouazzani, E. Michel, R. Aznar, G. Porte, and J. Appell, J. Phys. Chem. B **105**, 10 528 (2001).
[16] J. Israelachvili, *Intermolecular and Surface Forces*, 2nd ed. (Academic Press, London, 1991), p. 354.

[17] D. Chatenay, W. Urbach, A.M. Cazabat, and D. Langevin, Phys. Rev. Lett. **54**, 2253 (1985).
[18] D. Chatenay, W. Urbach, R. Messager, and D. Langevin, J. Chem. Phys. **86**, 2343 (1987).
[19] J. Narayanan, W. Urbach, D. Langevin, C. Manohar, and R. Zana, Phys. Rev. Lett. **81**, 228 (1998).
[20] D. Stauffer, *Introduction to Percolation Theory* (Taylor & Francis, London, 1985).